

# Host Adaptation of a Bacterial Toxin from the Human Pathogen *Salmonella* Typhi

Lingquan Deng,<sup>1,2,4,8</sup> Jeongmin Song,<sup>5,8,9</sup> Xiang Gao,<sup>5,8</sup> Jiawei Wang,<sup>6</sup> Hai Yu,<sup>7</sup> Xi Chen,<sup>7</sup> Nissi Varki,<sup>1,3</sup> Yuko Naito-Matsui,<sup>1,2,4</sup> Jorge E. Galán,<sup>5,\*</sup> and Ajit Varki<sup>1,2,3,4,\*</sup>

<sup>1</sup>Glycobiology Research and Training Center

<sup>2</sup>Department of Medicine

<sup>3</sup>Department of Pathology

<sup>4</sup>Department of Cellular and Molecular Medicine

University of California, San Diego, La Jolla, CA 92093, USA

<sup>5</sup>Department of Microbial Pathogenesis, Yale University School of Medicine, New Haven, CT 06536, USA

<sup>6</sup>School of Life Sciences, Tsinghua University, Beijing 100084, PRC

<sup>7</sup>Department of Chemistry, University of California, Davis, Davis, CA 95616, USA

<sup>8</sup>Co-first author

<sup>9</sup>Present address: Department of Microbiology and Immunology, Cornell University College of Veterinary Medicine, Ithaca, NY 14853, USA

\*Correspondence: [jorge.galan@yale.edu](mailto:jorge.galan@yale.edu) (J.E.G.), [a1varki@ucsd.edu](mailto:a1varki@ucsd.edu) (A.V.)

<http://dx.doi.org/10.1016/j.cell.2014.10.057>

## SUMMARY

*Salmonella* Typhi is an exclusive human pathogen that causes typhoid fever. Typhoid toxin is a *S. Typhi* virulence factor that can reproduce most of the typhoid fever symptoms in experimental animals. Toxicity depends on toxin binding to terminally sialylated glycans on surface glycoproteins. Human glycans are unusual because of the lack of CMAH, which in other mammals converts N-acetylneuraminic acid (Neu5Ac) to N-glycolylneuraminic acid (Neu5Gc). Here, we report that typhoid toxin binds to and is toxic toward cells expressing glycans terminated in Neu5Ac (expressed by humans) over glycans terminated in Neu5Gc (expressed by other mammals). Mice constitutively expressing CMAH thus displaying Neu5Gc in all tissues are resistant to typhoid toxin. The atomic structure of typhoid toxin bound to Neu5Ac reveals the structural bases for its binding specificity. These findings provide insight into the molecular bases for *Salmonella* Typhi's host specificity and may help the development of therapies for typhoid fever.

## INTRODUCTION

*Salmonella enterica* serovar Typhi (*S. Typhi*), the cause of typhoid fever, continues to be a major public health concern, particularly in developing countries. There are more than 20 million cases of typhoid fever every year, which result in more than 400,000 deaths (Crump and Mintz, 2010; Parry and Threlfall, 2008; Voetsch et al., 2004). Unlike the illnesses associated with most other *Salmonella*, which are usually self-limiting gastroenteritis (i.e., “food poisoning”), typhoid fever is a systemic, often lethal disease (Parry et al., 2002). In addition, in contrast to most *Salmonella enterica* serovars, which can infect

a broad range of hosts, *S. Typhi* exhibits remarkable host specificity, causing symptomatic infections only in humans (Ohl and Miller, 2001; Parry et al., 2002; Raffatellu et al., 2008). The mechanisms of *S. Typhi* host specificity are incompletely understood and most likely multifactorial. For example, *S. Typhi* is unable to replicate in most hosts, except chimpanzees where it was found to reach levels equivalent to those in humans (Edsall et al., 1960; Metchnikoff and Besredka, 1911). However, despite significant bacterial replication, *S. Typhi* did not cause typical typhoid fever symptoms in chimpanzees, which developed a milder and much shorter lasting disease syndrome (Edsall et al., 1960; Metchnikoff and Besredka, 1911). These observations indicate that in addition to pathogen restriction, there are other host factors that must prevent the development of typhoid fever even in the presence of significant bacterial replication. Host restriction is manifested at the cellular level because, in contrast to human macrophages, *S. Typhi* is unable to survive within macrophages of nonpermissive species (Schwan et al., 2000; Vladioianu et al., 1990). Recent studies have identified a Rab32-dependent pathogen-restriction mechanism that limits the growth of *S. Typhi* within macrophages of nonpermissive species (Spanò and Galán, 2012). In contrast, this antimicrobial function is effectively neutralized by broad-host *Salmonella* serovars, which are able to proteolytically target Rab32 with a type III secretion effector protein that is absent from *S. Typhi* (Spanò and Galán, 2012; Spanò et al., 2011).

Typhoidal (i.e., able to cause typhoid fever) *Salmonella* serovars (e.g., *S. Typhi* and *S. Paratyphi*) encode typhoid toxin, a unique member of the AB<sub>5</sub> exotoxin family (Haghjoo and Galán, 2004; Song et al., 2013; Spanò et al., 2008). Unlike all known members of this family, which possess a single enzymatic A subunit associated to a pentameric B subunit (Beddoe et al., 2010), typhoid toxin is composed of two covalently linked enzymatic subunits, the deoxyribonuclease CdtB and the ADP ribosyl transferase PliA, associated to the homopentameric B subunit PliB (Song et al., 2013). Thus typhoid toxin may have evolved from the combination of two exotoxins, cytolethal distending and pertussis toxins, and is the only known example of a toxin

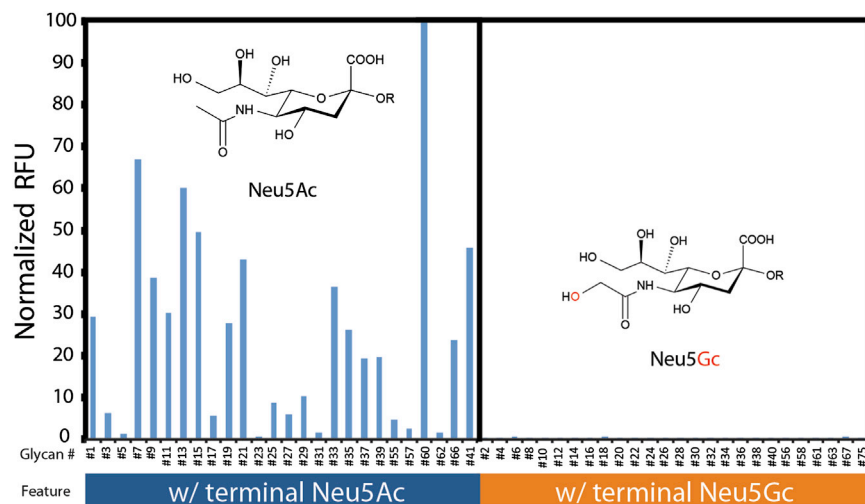


**Figure 1. Comparison of Typhoid Toxin Binding to Paired Neu5Ac- and Neu5Gc-Terminated Glycans by a Customized Microarray**

Chemical structures of Neu5Ac and Neu5Gc are shown. The two molecules differ by only one single oxygen atom. Vertical axis values represent the normalized average of relative fluorescence units and horizontal axis indicates the glycan number in the array.

See also [Figure S1](#) and [Tables 1](#) and [S1](#).

with an A<sub>2</sub>B<sub>5</sub> organization. Recent studies have shown that direct injection of typhoid toxin into experimental animals can reproduce many of the pathognomonic symptoms of typhoid fever, thus placing this toxin at the center of the pathogenesis of this devastating disease ([Song et al., 2013](#)).

To enter cells typhoid toxin must bind glycosylated surface glycoprotein receptors in target cells, such as podocalyxin 1 on epithelial cells and CD45 on myelocytic cells ([Song et al., 2013](#)). The toxin recognizes specific sialylated glycan moieties on the receptor proteins through a glycan-binding domain in its PltB B subunit. Sialoglycans on human cells are unusual in that they are primarily terminated in *N*-acetylneuraminic acid (Neu5Ac) ([Varki et al., 2011](#)). This is in contrast to other old world primates and most other mammals studied to date, whose glycans can also terminate in *N*-glycolylneuraminic acid (Neu5Gc). These differences in glycan composition are the result of the absence of CMP-*N*-acetylneuraminic acid hydroxylase (CMAH) in humans, due to an Alu-mediated exon deletion in the *CMAH* gene, which occurred after the separation of the *Hominin* lineage from other Hominids (the so-called “great apes,” e.g., chimpanzees) ([Chou et al., 2002](#)). Here, we report that typhoid toxin exhibits exquisite specificity for human-like Neu5Ac-terminated glycans. We find that typhoid toxin is cytotoxic to cells expressing Neu5Ac glycans on their surface but not to those expressing Neu5Gc. Furthermore, typhoid toxin binds strongly to human tissues but poorly to those from chimpanzees, which predominantly display Neu5Gc-terminated glycans and do not develop the typical symptoms of typhoid fever. We also show that mice engineered to display Neu5Gc glycans in all tissues are resistant to typhoid toxin. These findings provide major insight into the molecular bases for the host specificity of *S. Typhi* and may help the development of novel therapeutic approaches against typhoid fever.

## RESULTS

### Typhoid Toxin Exhibits Strong Specificity for Neu5Ac-Terminated Glycans

Given the remarkable human specificity exhibited by *S. Typhi* and the central role of typhoid toxin in the pathogenesis of

typhoid fever, we used a customized glycan array ([Padler-Karavani et al., 2014](#)) to compare the ability of fluorescently labeled typhoid toxin to bind pairs of sialylated glycans terminated in either Neu5Ac (predominantly expressed in human cells) or Neu5Gc (predominantly expressed in cells of most other mammals). Consistent with previous results ([Song et al., 2013](#)), typhoid toxin bound a diverse group of sialylated glycans with preferential binding to termini with the consensus sequence Neu5Ac $\alpha$ 2-3Gal $\beta$ 1-3/ $\beta$ 1-4Glc/GlcNAc ([Figure 1](#); [Table 1](#); [Table S1](#) available online). Remarkably, however, we found that typhoid toxin did not bind to otherwise identical glycans terminated in Neu5Gc (i.e., differing by a single oxygen atom) ([Figures 1](#) and [S1](#); [Table 1](#); [Table S1](#)). The marked difference in binding was observed across all the glycans tested and with different toxin concentrations ([Table 1](#); [Figure S1](#); [Table S1](#)). Consistent with previous observations ([Song et al., 2013](#)), typhoid toxin carrying a mutation in the glycan-binding site of its PltB B subunit (PltB<sup>S35A</sup>) did not show significant binding to any of the glycans tested regardless of their sialylation status ([Table S1](#)). To confirm typhoid toxin’s preference for Neu5Ac-terminated glycans, we compared its binding to human and chimpanzee red blood cells, which display markedly different levels of surface Neu5Ac or Neu5Gc-terminated glycans ([Figure 2A](#)). In keeping with the glycan array findings, typhoid toxin showed much stronger binding to human than to chimpanzee cells ([Figure 2B](#)). Furthermore, the differences were observed at different toxin concentrations ([Figure 2B](#)). Similar differences were observed with lymphocytes from humans and chimpanzees ([Figures 2C](#) and [2D](#)). These results indicate that typhoid toxin exhibits strong binding preference for Neu5Ac-terminated glycans, which are predominant in human cells.

### Incorporation of Neu5Gc Renders Human Cells Resistant to Typhoid Toxin

Although human cells lack Neu5Gc, they can metabolically incorporate this sialic acid if supplied into the cell culture medium ([Tangvoranuntakul et al., 2003](#)). To investigate the biological significance of typhoid toxin glycan selectivity, we compared the binding of fluorescently labeled typhoid toxin to human Henle-407 epithelial cells that had been grown in media supplemented with Neu5Gc or Neu5Ac. Predictably, growth in the presence of Neu5Gc significantly altered the sialic acid composition in these cells resulting in up to 60% of the total sialic acid containing

**Table 1. Analysis of Fine Ligand Specificity of Native Typhoid Toxin by a Customized Sialoglycan Microarray**

Glycan Structure	Mean Relative Fluorescence Units (n = 4)	
	Sia = Neu5Ac	Sia = Neu5Gc
Sia $\alpha$ 3Gal $\beta$ 3GlcNAc $\beta$ 3Gal $\beta$ 4Glc $\beta$ O(CH <sub>2</sub> ) <sub>3</sub> NH <sub>2</sub>	34,441	25
Sia9Ac $\alpha$ 3Gal $\beta$ 3GlcNAc $\beta$ O(CH <sub>2</sub> ) <sub>3</sub> NH <sub>2</sub>	23,120	73
Sia $\alpha$ 3Gal $\beta$ 3GlcNAc $\beta$ O(CH <sub>2</sub> ) <sub>3</sub> NH <sub>2</sub>	20,664	156
Sia $\alpha$ 3Gal $\beta$ 3GalNAc $\alpha$ O(CH <sub>2</sub> ) <sub>3</sub> NH <sub>2</sub>	17,100	88
Sia $\alpha$ 8Sia $\alpha$ 3Gal $\beta$ 4Glc $\beta$ O(CH <sub>2</sub> ) <sub>3</sub> NH <sub>2</sub>	15,821	134
Sia $\alpha$ 3Gal $\beta$ 4Glc $\beta$ O(CH <sub>2</sub> ) <sub>3</sub> NH <sub>2</sub>	14,781	108
Sia9Ac $\alpha$ 3Gal $\beta$ 3GalNAc $\alpha$ O(CH <sub>2</sub> ) <sub>3</sub> NH <sub>2</sub>	13,299	42
Sia $\alpha$ 3Gal $\beta$ 3GalNAc $\beta$ O(CH <sub>2</sub> ) <sub>3</sub> NH <sub>2</sub>	12,564	147
Sia $\alpha$ 3Gal $\beta$ 4GlcNAc $\beta$ O(CH <sub>2</sub> ) <sub>3</sub> NH <sub>2</sub>	10,468	114
Sia9Ac $\alpha$ 3Gal $\beta$ 4GlcNAc $\beta$ O(CH <sub>2</sub> ) <sub>3</sub> NH <sub>2</sub>	10,076	30
Sia $\alpha$ 6Gal $\beta$ 4Glc $\beta$ O(CH <sub>2</sub> ) <sub>3</sub> NH <sub>2</sub>	9,605	79
Sia9Ac $\alpha$ 3Gal $\beta$ 3GalNAc $\beta$ O(CH <sub>2</sub> ) <sub>3</sub> NH <sub>2</sub>	8,993	72
Sia $\alpha$ 3(Neu5Ac $\alpha$ 6)Gal $\beta$ 4Glc $\beta$ O(CH <sub>2</sub> ) <sub>3</sub> NH <sub>2</sub>	8,205	246
Sia9Ac $\alpha$ 3Gal $\beta$ 4Glc $\beta$ O(CH <sub>2</sub> ) <sub>3</sub> NH <sub>2</sub>	6,730	76
Sia9Ac $\alpha$ 6Gal $\beta$ 4Glc $\beta$ O(CH <sub>2</sub> ) <sub>3</sub> NH <sub>2</sub>	6,619	56
Sia9Ac $\alpha$ 3Gal $\beta$ O(CH <sub>2</sub> ) <sub>3</sub> NH <sub>2</sub>	3,513	152
Sia $\alpha$ 3Gal $\beta$ O(CH <sub>2</sub> ) <sub>3</sub> NH <sub>2</sub>	3,040	182
Sia9Ac $\alpha$ 6Gal $\beta$ 4GlcNAc $\beta$ O(CH <sub>2</sub> ) <sub>3</sub> NH <sub>2</sub>	2,160	89
Sia $\alpha$ 6Gal $\beta$ O(CH <sub>2</sub> ) <sub>3</sub> NH <sub>2</sub>	2,078	125
Sia $\alpha$ 6Gal $\beta$ 4GlcNAc $\beta$ O(CH <sub>2</sub> ) <sub>3</sub> NH <sub>2</sub>	1,979	229
Sia $\alpha$ 3Gal $\beta$ 4(Fuc $\alpha$ 3)GlcNAc $\beta$ O(CH <sub>2</sub> ) <sub>3</sub> NH <sub>2</sub>	1,633	51
Sia $\alpha$ 3Gal $\beta$ 4(Fuc $\alpha$ 3)GlcNAc6S $\beta$ O(CH <sub>2</sub> ) <sub>3</sub> NH <sub>2</sub>	827	96
Sia9Ac $\alpha$ 6Gal $\beta$ O(CH <sub>2</sub> ) <sub>3</sub> NH <sub>2</sub>	592	133
Sia $\alpha$ 3Gal $\beta$ 4GlcNAc6S $\beta$ O(CH <sub>2</sub> ) <sub>3</sub> NH <sub>2</sub>	511	80
Sia $\alpha$ 6GalNAc $\alpha$ O(CH <sub>2</sub> ) <sub>3</sub> NH <sub>2</sub>	470	200
Sia9Ac $\alpha$ 6GalNAc $\alpha$ O(CH <sub>2</sub> ) <sub>3</sub> NH <sub>2</sub>	217	49

Neu5Gc (Figure 3A). In contrast, cells grown in standard media or supplemented with Neu5Ac had almost undetectable levels of Neu5Gc (Figure 3A). Consistent with its reduced binding affinity to Neu5Gc terminated glycans, typhoid toxin binding and toxicity was markedly reduced in cells grown in the presence of Neu5Gc (Figures 3B–3D and S2). In contrast, levels of toxin binding and cytotoxicity were slightly increased in cells grown in media supplemented with Neu5Ac in comparison to cells grown in standard media (Figures 3B–3D and S2). Equivalent results were observed in Jurkat T cells, which display a different glycoprotein receptor for typhoid toxin (Song et al., 2013) (Figures 3E–3H). These results indicate that the abundance of Neu5Gc on the surface glycans render cells less permissive for toxin binding and therefore resistant to typhoid toxin.

### Constitutive Expression of Neu5Gc Renders Mice Resistant to Typhoid Toxin

Although wild-type mice express a fully functional CMAH and can express Neu5Gc, most of their tissues contain a significant amount of Neu5Ac as well, presumably due to low expression

of CMAH in some cells (Hedlund et al., 2007). Consistent with this observation, *Cmah*<sup>-/-</sup> mice (Hedlund et al., 2007) did not exhibit significantly higher susceptibility to typhoid toxin, showing equivalent levels of weight loss, white blood cell depletion, and time to death compared to those observed in wild-type animals (Figures 4A–4D). In fact, these mice exhibited a slightly reduced susceptibility to the toxin, which is most likely due to the presence of high levels of Neu5Ac-containing glycoproteins in the sera of these animals, which may provide protection against toxicity by competing with toxin binding to tissue receptors (Beddoe et al., 2010). We therefore tested the susceptibility to typhoid toxin of mice engineered to constitutively overexpress CMAH in all tissues (*Cmah*<sup>tg</sup>) (Figures 4A–4D). We reasoned that the forced expression of CMAH would result in the predominant display of Neu5Gc on the surface of all cells and thus confer protection against intoxication. Consistent with this hypothesis, *Cmah*<sup>tg</sup> mice were completely resistant to systemic administration of toxin amounts much higher than those that would be lethal for wild-type mice (Figure 4D). Also consistent with these observations, the binding of fluorescently labeled typhoid toxin was undetectable in tissues from *Cmah*<sup>tg</sup> mice but was readily detectable in tissues from wild-type and *Cmah*<sup>-/-</sup> mice (Figure S3).

### Typhoid Toxin Does Not Bind to Chimpanzee Tissues

Previous studies have shown that chimpanzees can be experimentally infected with *S. Typhi* (Edsall et al., 1960; Metchnikoff and Besredka, 1911). However, infected animals did not develop the typical symptomatology associated with typhoid fever, such as the presence of stupor and extreme lethargy, showing instead a course of disease that was mild and brief. We found that, contrary to human tissues, toxin binding to chimpanzee organ tissue sections was nondetectable (Figure 5). This is explained by the observation that chimpanzee cells predominantly display Neu5Gc-terminated glycans on their surface and are therefore not permissive for toxin binding. These results are consistent with the hypothesis that the lack of pathognomonic typhoid fever symptomatology observed in chimpanzees experimentally infected with *S. Typhi* is due to the inability of typhoid toxin to gain access to target cells.

### The Crystal Structure of Typhoid Toxin B Subunit PltB Bound to Its Sialic Acid Ligand Reveals Structural Bases for Its Binding Specificity

To gain insight into the structural bases for typhoid toxin's binding specificity, we determined the atomic structure at 1.92 Å resolution of PltB bound to GalNAc $\beta$ 1-4(Neu5Ac $\alpha$ 2-8Neu5Ac $\alpha$ 2-3)Gal $\beta$ 1-4Glc (Figures 6A and 6B; Table S2), which previous studies have shown binds typhoid toxin with high affinity (Song et al., 2013). Clear electron density corresponding to the (Neu5Ac $\alpha$ 2-8Neu5Ac $\alpha$ 2-3)Gal trisaccharide was unambiguously observed at the canonical glycan-binding sites in two of the five subunits of the PltB pentamer (Figures 6A–6C). Because the glycan-binding sites of every subunit are identical, absence of binding to some subunits is most likely due to their limited accessibility because of crystal packing. No specific contacts between the galactose moiety and PltB were observed in the structure (Figure S4). In contrast, the first of the two Neu5Ac moieties interacts through multiple direct hydrogen bonds and

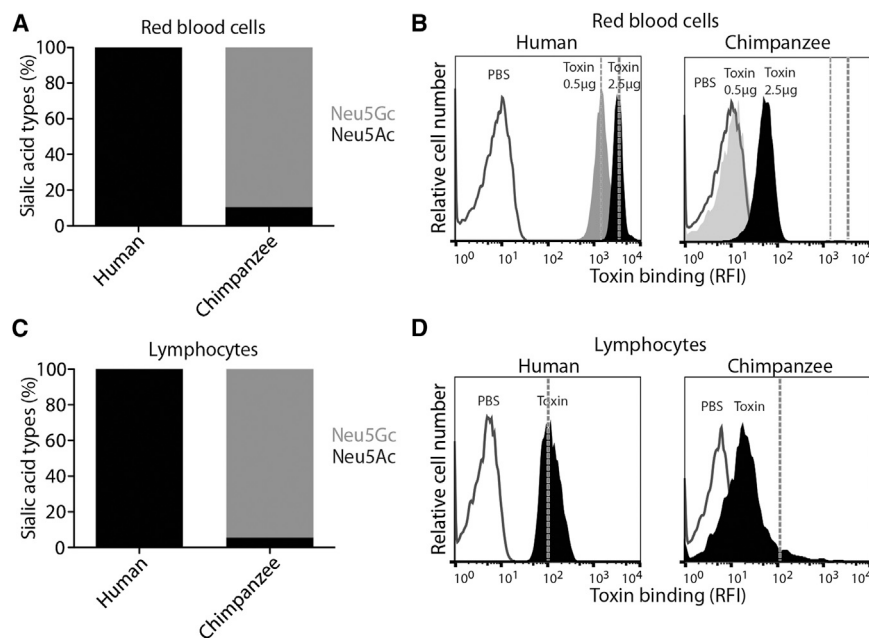


**Figure 2. Typhoid Toxin Binding to Red Blood Cells and Lymphocytes from Humans and Chimpanzees**

(A) Relative levels of Neu5Ac/Neu5Gc in human and chimpanzee red blood cells (RBCs).

(B) Binding of different amounts of typhoid toxin to human and chimpanzee RBCs.

(C) Relative levels of Neu5Ac/Neu5Gc in human and chimpanzee lymphocytes.

(D) Binding of typhoid toxin to human and chimpanzee lymphocytes. Similar results were obtained in several independent repetitions of the experiments. RFI, relative fluorescence intensity. PBS, phosphate buffered saline.

and suggest an evolutionary pathway by which this toxin restricted its binding to human-specific glycans.

## DISCUSSION

Unlike most other *Salmonella enterica* serovars, which can infect a broad range of hosts, *S. Typhi* can only infect humans, in

whom it causes typhoid fever, a severe, often lethal disease. The process by which *S. Typhi* has lost its ability to explore other niches and evolved to cause disease only in humans is incompletely understood and likely to be multifactorial (Jacobson et al., 2011; Sabbagh et al., 2010). The *S. Typhi* genome sequence exhibits an unusually high number of pseudogenes, suggesting that genome reduction most likely played a central role in its adaptation to a single host (Parkhill et al., 2001). For example, the interaction of *Salmonella enterica* with host cells is largely dictated by two type III secretion systems (T3SS), which deliver bacterial effector proteins into host cells to modulate cellular functions (Galán, 2001; Ibarra and Steele-Mortimer, 2009; Srikanth et al., 2011; Waterman and Holden, 2003). Although these systems are highly conserved across different *Salmonella* serovars, the effectors they deliver are not, and *S. Typhi* expresses a significantly smaller number of effector proteins than most other serovars. One of the missing effectors from *S. Typhi* is GtgE, which is involved in neutralizing a host restriction pathway that prevents its growth in macrophages of nonpermissive species (Spanò et al., 2011).

*S. Typhi* host specificity, however, is not exclusively due to its inability to replicate within nonpermissive hosts. For example, unlike mice, chimpanzees were found to be permissive for *S. Typhi* replication, and experimental infections showed that in these animals it reached levels equivalent to those observed in infected humans (Edsall et al., 1960; Metchnikoff and Besredka, 1911). However, chimpanzees did not develop the typical symptomatology of typhoid fever indicating that factors other than pathogen restriction contribute to *S. Typhi*'s host specificity. Previous studies have shown that typhoid toxin is central for the development of pathognomonic symptoms of typhoid fever (Song et al., 2013). We have shown here that typhoid toxin exhibits strong selectivity for Neu5Ac-terminated glycans, predominantly expressed in human cells, over Neu5Gc-terminated

water-mediated hydrogen bonds with Tyr33, Ser35, Lys59, Thr65, and Arg100 in PltB (Figure 6D). In addition, the first Neu5Ac sugar ring makes hydrophobic contacts with the aromatic rings of Tyr33 and Tyr34. The second Neu5Ac contacts PltB through direct and water-mediated hydrogen bonds with Ser35, Asp36, Lys59, Asn61, Ser63, Ala130, and Thr131 of the glycan-binding domain (Figure S4). Consistent with their importance in carbohydrate binding, mutations in Tyr33, Ser35, and Lys59 drastically disrupted typhoid toxin activity (Figures 6E and S5). Some toxin B subunits undergo conformational changes upon binding their glycan receptors (Sixma et al., 1992). To investigate this possibility, we solved the atomic structure of the apo form of PltB at 2.08 Å resolution. Comparison of the atomic structures of the receptor-bound and apo forms of PltB indicates that binding to glycan receptors does not result in marked conformational changes in PltB (Figure S6).

Typhoid toxin's PltB shares its oligosaccharide-binding fold with the B subunits of other AB<sub>5</sub> toxins such as subtilase cytoxin's SubB (Byres et al., 2008; Song et al., 2013). However, SubB exhibits the opposite specificity, strongly favoring binding to Neu5Gc-terminated glycans (Byres et al., 2008). Therefore, comparison of the atomic structures of PltB and SubB bound to their glycan receptors afforded us an opportunity to obtain insight into the structural bases for the binding specificity. The arrangement of the main chain of Neu5Ac relative to the binding pocket of PltB is very similar to that of Neu5Gc bound to SubB (Byres et al., 2008), and many of the critical interactions between the glycans and specific residues of PltB and SubB are conserved (Figure 6F). However, a residue equivalent to Tyr78 in SubB, which forms a critical hydrogen bond with the extra hydroxyl group in Neu5Gc is missing from PltB (Figure 6F). Instead, at this position PltB has the nonpolar residue Val103 and thus is unable to interact with Neu5Gc. These findings provide a structural explanation for typhoid toxin's inability to bind Neu5Gc-terminated glycans

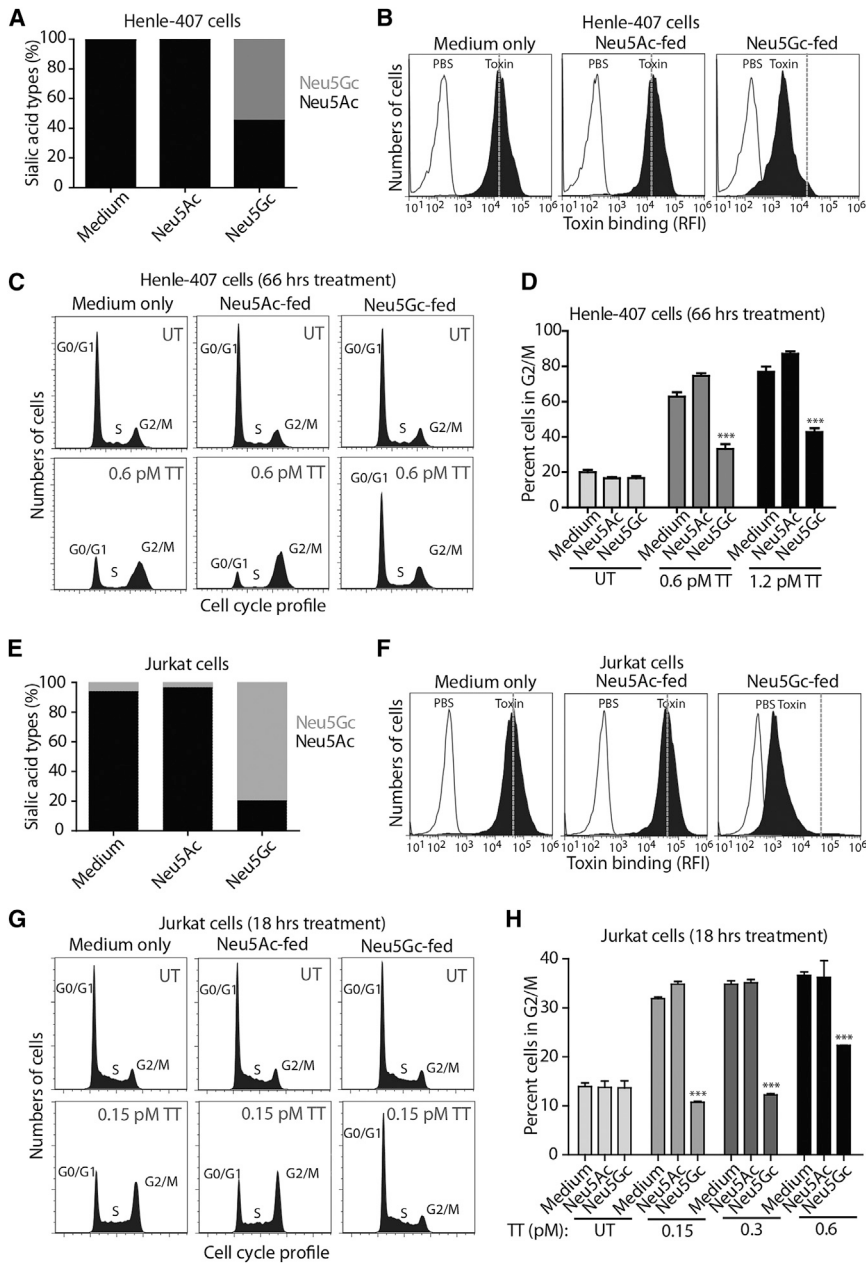


**Figure 3. Typhoid Toxin Binds to and Is Cytotoxic toward Cells Displaying Neu5Ac-, But Not to Those Displaying Neu5Gc-, Terminated Glycans**

Human intestinal epithelial Henle-407 cells (A–D) and human T lymphocyte Jurkat cells (E–H) were left untreated (medium only) or fed Neu5Ac or Neu5Gc in a culture medium for 4 days. Cells were then analyzed by HPLC to examine their relative sialic acid composition (A and E), or used in typhoid toxin binding (B and F) and toxicity assays by examining the cell cycle profile of toxin-treated cells (C, D, G, and H). Data in (D) and (H) are the mean ± SEM; \*\*\*p < 0.0001, compared to the percent of control (medium-treated) cells in G2/M in the same group. See also Figure S2.

lase B subunit SubB bound to Neu5Gc with the structure of PltB bound to Neu5Ac revealed that the arrangement of the main chain of the two glycans relative to their binding pockets is very similar and many of the critical interactions between the glycans and specific residues of PltB and SubB are highly conserved. However, PltB lacks a residue equivalent to Tyr78 in SubB, which forms a critical hydrogen bond with the extra hydroxyl group in Neu5Gc. Because in all likelihood PltB evolved from a Neu5Gc-binding ancestor, this finding suggests that only subtle changes in the glycan-binding site would have been necessary to drastically change typhoid toxin's binding specificity and host range. However, mutagenesis analysis of PltB suggests a more complex picture since changing Val103 to Tyr in PltB (equivalent to Tyr78 in SubB) resulted in a loss of function rather than in a change in binding specificity (Figure S7). Additional structures of PltB bound to different glycans will be required to fully understand the evolution of typhoid toxin's exquisite binding specificity.

glycans, which are predominantly expressed by most other mammals. Therefore, the exquisite binding selectivity of typhoid toxin for glycans predominantly expressed in human cells provides an explanation for the inability of *S. Typhi* to cause typhoid fever in some nonpermissive species like chimpanzees, which allow significant bacterial replication.

The extreme specificity for human glycans exhibited by typhoid toxin is striking and unprecedented among bacterial toxins. The bacterial toxin subtilase, expressed by some strains of *E. coli*, exhibits the opposite specificity and its B subunit strongly favors binding to Neu5Gc-terminated glycans (Byres et al., 2008), which is consistent with the broad host specificity of this pathogen. Comparison of the crystal structures of subti-

lase B subunit SubB bound to Neu5Gc with the structure of PltB bound to Neu5Ac revealed that the arrangement of the main chain of the two glycans relative to their binding pockets is very similar and many of the critical interactions between the glycans and specific residues of PltB and SubB are highly conserved. However, PltB lacks a residue equivalent to Tyr78 in SubB, which forms a critical hydrogen bond with the extra hydroxyl group in Neu5Gc. Because in all likelihood PltB evolved from a Neu5Gc-binding ancestor, this finding suggests that only subtle changes in the glycan-binding site would have been necessary to drastically change typhoid toxin's binding specificity and host range. However, mutagenesis analysis of PltB suggests a more complex picture since changing Val103 to Tyr in PltB (equivalent to Tyr78 in SubB) resulted in a loss of function rather than in a change in binding specificity (Figure S7). Additional structures of PltB bound to different glycans will be required to fully understand the evolution of typhoid toxin's exquisite binding specificity. Nevertheless, from the host perspective, it is remarkable that a single oxygen atom could have such a dramatic impact on pathogenicity.

We have shown here that a toxin produced by a human-specific pathogen has evolved to selectively bind human sialoglycans. This is a remarkable example of virulence factor adaptation to a specific host that provides major insight into the process of host adaptation of the human pathogen *S. Typhi*. Given typhoid toxin's central role in the development of typhoid fever, these observations provide the bases for novel therapeutic strategies and may help the development of an animal model for the study of typhoid fever and the pathogenesis of typhoid toxin.

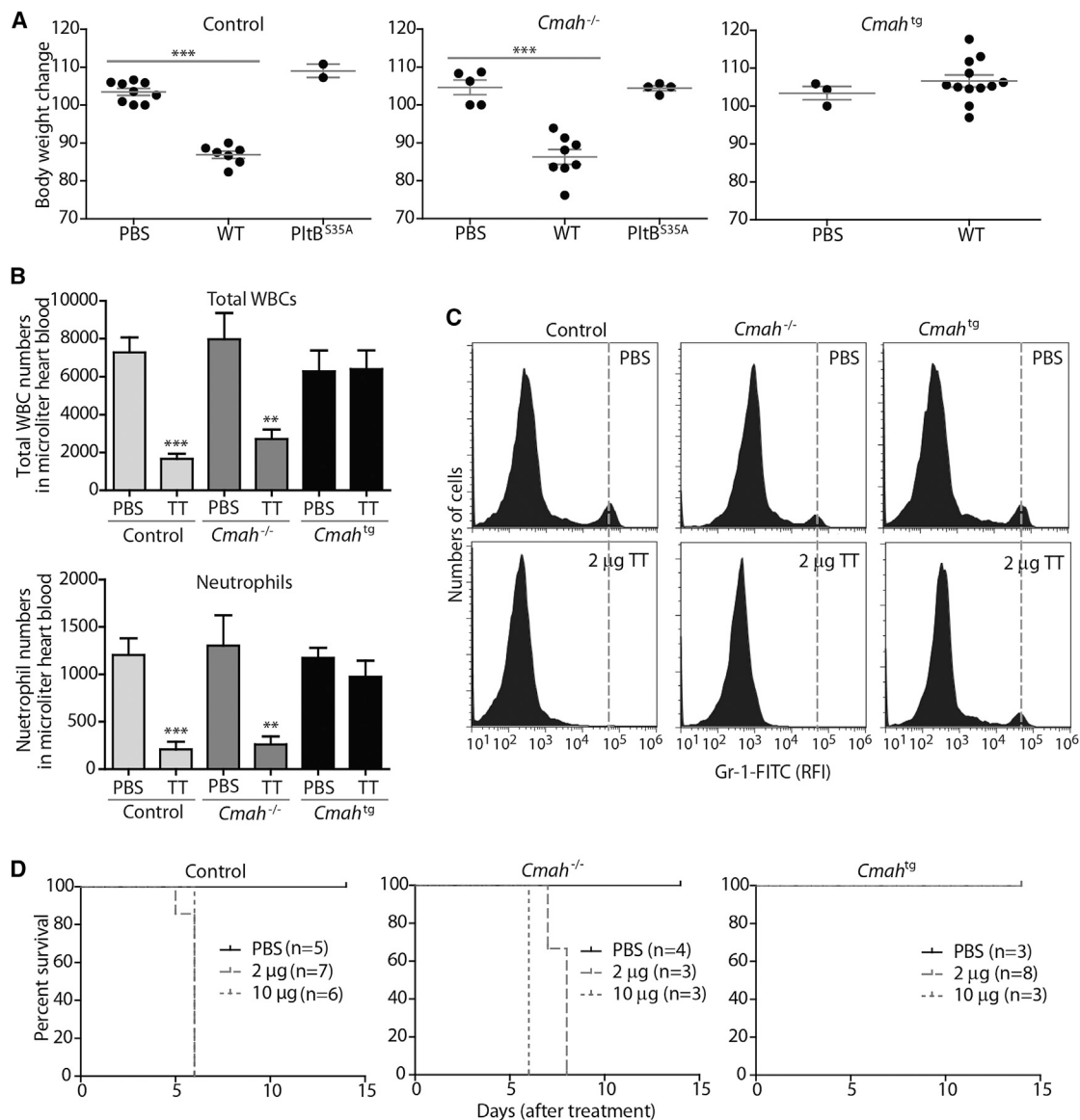


#### Figure 4. Mice Engineered to Constitutively Express CMAH, Resulting in Elevated Levels of Neu5Gc in All Tissues, Are Resistant to Typhoid Toxin

Purified preparations of wild-type typhoid toxin or a binding-defective mutant (PitB<sup>S35A</sup>) were systemically administered into mice defective in (*Cmah*<sup>-/-</sup>) or constitutively expressing CMAH (*Cmah*<sup>tg</sup>) or control (C57BL/6) mice.

(A–C) Four days after treatment their total weight (A) and the total number of white cells (WBC) (B, top panel) or neutrophils (B, bottom) were measured as indicated in [Experimental Procedures](#). Black circles represent the percentage of the weight of an animal relative to its weight immediately before treatment (A). Circulating white blood cells were counted in a hematology analyzer (B). Alternatively, peripheral blood cells from animals that had received the indicated treatments were stained with an antibody directed to the neutrophil cell marker Gr1 and the number of stained cells was determined by flow cytometry (C). The histograms shown are from ungated samples. Similar results were obtained in several independent repetitions of the experiment. RFI, relative fluorescence intensity. TT, typhoid toxin. WT, wild-type. Data in (B) are the mean  $\pm$  SEM; \*\*\* $p < 0.0001$ , \*\* $p < 0.002$  (relative to the buffer control in the same group).

(D) Survival of mice after administration of different amounts of typhoid toxin. PBS, phosphate buffered saline. The difference in the survival curves of PBS versus toxin-treated (all concentrations) control and *Cmah*<sup>-/-</sup> animals was statistically significant ( $p < 0.001$ ; log-rank Mantel-Cox test). The difference between the survival curves in control and *Cmah*<sup>-/-</sup> mice after administration of 2  $\mu$ g of toxin was statistically significant ( $p < 0.001$ ). However, after administration of 10  $\mu$ g of toxin the difference between the survival curves in control and *Cmah*<sup>-/-</sup> mice was not statistically significant ( $p < 0.6$ ).

See also [Figure S3](#).

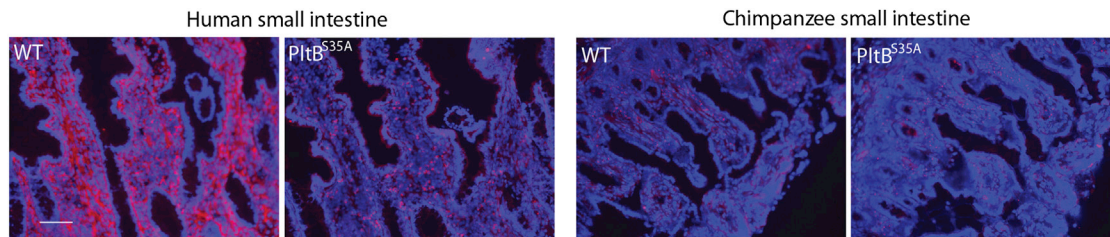


**Figure 5. Typhoid Toxin Does Not Bind to Chimpanzee Tissues**

Frozen sections of small intestine from humans or chimpanzees were stained with fluorescently labeled typhoid toxin or its binding-defective PitB<sup>S35A</sup> mutant (red) and counterstained with Hoechst (blue). Scale bar represents 100  $\mu\text{m}$ .

## EXPERIMENTAL PROCEDURES

### Typhoid Toxin Expression and Purification

Expression and purification of typhoid toxin was carried out as previously described (Song et al., 2013). Plasmids expressing PitB point mutations were constructed using standard recombinant DNA techniques.

### Crystallization

Expression and purification of C-terminal 6 $\times$  His-tagged PitB used for crystallization have been described previously (Song et al., 2013). Initial sparse matrix crystallization trials of full-length PitB protein preparations (5.5 mg ml<sup>-1</sup>) were carried out at the Yale University School of Medicine Structural Biology Core facility. After crystal optimization trials, full-length PitB crystals appeared in 2 to 3 days and matured in  $\sim$ 1 week at room temperature using the hanging-drop vapor-diffusion method in a mix of 1  $\mu\text{l}$  of protein with 1  $\mu\text{l}$  of reservoir solution consisting of 26% (w/v) PEG1500 and 0.1 M sodium acetate, pH5.0. Native PitB crystals were soaked by the addition of GD2 in different concentrations (from 1 mM to 50 mM). In most cases, the crystals broke upon addition of the sugar, even at sugar concentration of 1 mM. In very few cases, crystal debris large enough to be mounted on the X-ray source were obtained, which diffracted to  $\sim$ 3  $\text{\AA}$ .

### X-Ray Data Collection and Structure Determination

All data were collected at a wavelength of 1.5418  $\text{\AA}$  on a Rigaku Homelab system at the Yale University Chemical and Biophysical Instrumentation Center (CBIC) (<http://cbic.yale.edu>). Data were integrated and scaled using the HKL-2000 package (Otwinowski and Minor, 1997). Further processing was performed with programs from the CCP4 suite (Collaborative Computational Project, Number 4, 1994). The apo and GD2 bound PitB structures were both determined by molecular replacement using PHASER (McCoy et al., 2007) with the atomic coordinates of chain A of typhoid toxin (Song et al., 2013) (Protein Data Bank [PDB] ID 4K6L) as the initial search model. To complete the model, manual building was carried out in COOT (Emsley and Cowtan, 2004). Figures were prepared using PyMol (DeLano, 2002). The structure refinement was done by PHENIX (Adams et al., 2010). The data collection and refinement statistics are summarized in Table S2. Coordinates for the atomic structures have been deposited in the RCSB Protein Data Bank under PDB numbers 4RHR and 4RHS.

### Alexa 555 Typhoid Toxin Labeling

Purified wild-type and PitB<sup>S35A</sup> mutant typhoid toxins were fluorescently labeled with Alexa-555 (Invitrogen) according to the vendor's recommendation. Purified typhoid toxin preparations (1  $\mu\text{g}/\text{ml}$  in 500  $\mu\text{l}$  of 100 mM bicarbonate buffer) were incubated for 1 hr at room temperature (RT) with reactive dye and applied to a size exclusion chromatography column to separate dye-protein conjugates from free dye. Degree of labeling was determined by measuring the absorbance of the conjugate solution at 280 and 555 nm. Efficiency of labeling was equivalent for both wild-type and PitB<sup>S35A</sup> toxin preparations (4:1 dye/holotoxin ratio for both preparations). The typhoid holotoxin's predicted extinction coefficient is 191,400 M<sup>-1</sup> cm<sup>-1</sup>.

### Glycan Microarray Analysis

Glycan microarrays were fabricated using epoxide-derivatized glass slides as previously described (Padler-Karavani et al., 2014). Printed glycan microarray slides were blocked by ethanolamine, washed and dried, and then fitted in a multiwell microarray hybridization cassette (ArrayIt) to divide into subarrays. The subarrays were blocked with Ovalbumin (1% w/v) in PBS (pH 7.4) for 1 hr at RT in a humid chamber with gentle shaking. Subsequently, the blocking solution was discarded, and diluted wild-type or mutant typhoid toxin samples (Alexa Fluor 555-labeled) were added to each subarray. After incubating the toxins for 2 hr at RT with gentle shaking, the slides were extensively washed to remove nonspecifically bound proteins. The developed glycan microarray slides were then dried and subjected to scanning by a Genepix 4000B microarray scanner (Molecular Devices) immediately. Data analysis was done using the Genepix Pro 7.0 analysis software (Molecular Devices).

### Typhoid Toxin-Sialoglycan Binding Affinity Measured by Microscale Thermophoresis

The binding affinity of typhoid toxin to different glycans was measured using microscale thermophoresis as previously described (Wienken et al., 2010). Briefly, NT-647 fluorescently labeled typhoid toxin was incubated with a wide range of concentrations (12  $\mu\text{M}$  to 400 mM over 15 2-fold serial dilutions) of Neu5Ac $\alpha$ 2-3Gal $\beta$ 1-4Glc, at room temperature for 30 min in the dark. After equilibrium, the mixtures were loaded into 16 hydrophilic glass capillaries and the microscale thermophoresis analysis was performed using the Monolith NT.115 (Nano Temper). Data were analyzed and binding affinities were determined by the Nano Temper analysis software package. The sialoglycan underlying structure, Gal $\beta$ 1-4Glc (lactose), was used as a control under the same conditions.

### Mammalian Cell Culture Conditions

Henle-407 human intestinal epithelial and Jurkat human T lymphocyte cells were cultured in DMEM high glucose + 10% FBS and RPMI1640 + 10% FBS + 1 mM sodium pyruvate + 10 mM HEPES, respectively. All mammalian cells were kept at 37°C in a cell culture incubator with 5% CO<sub>2</sub>. Metabolic incorporation of Neu5Ac or Neu5Gc was carried out as previously described (Tangvoranuntakul et al., 2003). Briefly, cells were cultured in a standard medium supplemented with 10 mM Neu5Ac or 10 mM Neu5Gc (Inalco) as follows. Henle-407 ( $1.5 \times 10^6$ ) or Jurkat ( $1 \times 10^6$ ) cells were seeded into 12-well culture plates in 1 ml media with or without 10 mM sialic acid. A stock solution of 50 mM sialic acid was freshly prepared in a DMEM medium whose final pH was adjusted to neutral with NaOH. During the feeding period, the cells were continuously monitored and maintained below 80% confluence. After 3 days of growth, cells were split into 12-well plates at a cell density of  $1.5 \times 10^4$  (Henle-407) or  $1 \times 10^5$  (Jurkat) cells per well. The next day the cells were used for different assays as described below.

### High-Performance Liquid Chromatography

High-performance liquid chromatography (HPLC) analysis of sialic acids was carried out as previously described (Tangvoranuntakul et al., 2003). Briefly, sialic acids were released from glycans by hydrolysis with acetic acid, filtered

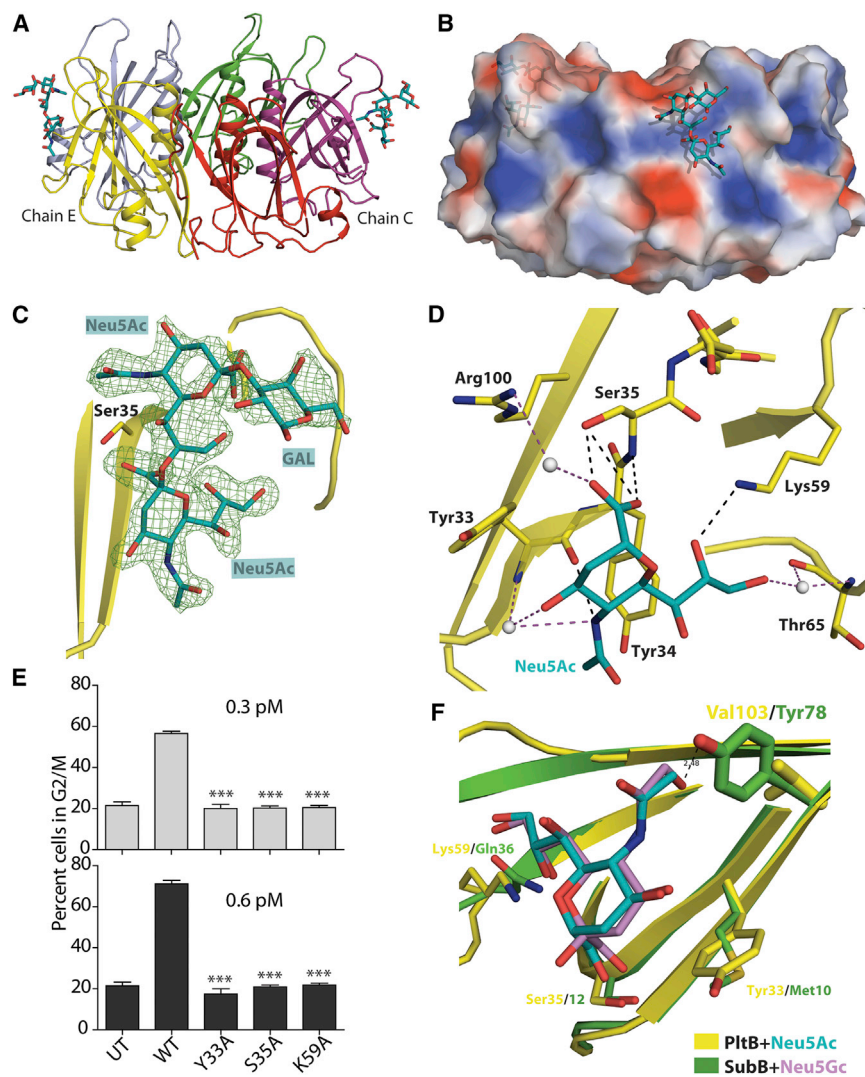


**Figure 6. Crystal Structure of Typhoid Toxin B Subunit PltB Bound to Its Sialic Acid Ligand**

(A) The atomic structure of the PltB pentamer in complex with the GalNAc $\beta$ 1-4(Neu5Ac $\alpha$ 2-8Neu5Ac $\alpha$ 2-3)Gal $\beta$ 1-4Glc oligosaccharide is shown as a ribbon cartoon with each protomer depicted in a different color. In the PltB pentamer, only partial oligosaccharide density (Neu5Ac-Neu5Ac-Gal) is seen in Chain C (purple) and E (yellow). Cyan sticks represent the sugar carbon atoms, blue sticks represent nitrogen atoms, and red sticks represent oxygen atoms.

(B) Surface charge distribution of the PltB pentamer structure and sugar-binding pockets.

(C) Close-up views of Neu5Ac-Neu5Ac-Gal and its composite annealed omit difference density map. PltB chain E and its key residue Ser35 are shown in yellow. Green mesh represents the sugar difference density map contoured at  $2.5\sigma$ .

(D) Interactions between PltB and Neu5Ac. Chain E of PltB is shown as a yellow colored ribbon cartoon, the amino acids interacting with the sugar are shown as sticks, and the direct interactions are shown in black dash. Water is shown as gray balls and water-mediated interactions are shown as purple dashes.

(E) Structure/function analysis of the PltB glycan-binding site. Typhoid holotoxin toxin preparations containing the indicated PltB mutants were tested for their ability to intoxicate cultured Henle-407 cells. Toxicity was evaluated by determining the percentage of cells arrested at the G2/M phase of the cell cycle, which is a measure of typhoid toxin's CdtB activity. Data are the mean  $\pm$  SEM; \*\*\* $p < 0.0001$ , compared to the percent cells treated with wild-type toxin that are in G2/M.

(F) Comparison of the sugar binding sites of PltB and SubB bound to Neu5Ac and Neu5Gc, respectively. Critical residues that differ between SubB (Tyr78) and PltB (Val103) are highlighted as sticks. Other interacting amino acids and sugars are shown in lines. PltB is shown in yellow, Neu5Ac in Cyan, SubB in Green, and Neu5Gc in light purple. See also Figures S4, S5, S6, and S7 and Table S2.

through a 10K Microcon filter unit (Millipore) and then derivatized by 1,2-diamino-4,5-methylene dioxybenzene (DMB) at  $50^{\circ}\text{C}$  for 2.5 hr in the dark. Resulting samples were analyzed by HPLC using a C18-column.

#### Typhoid Toxin Binding Assay

Cultured cells grown under different conditions (see above) were harvested, washed with Hank's balanced salt solution (HBSS), and resuspended in  $100\ \mu\text{l}$  HBSS containing 0.3 (for cultured Henle-407 or Jurkat cells) or  $0.5\ \mu\text{g}$  (for human and chimpanzee primary cells) of Alexa 555-labeled wild-type or mutant toxin preparations. Cells were incubated in the presence of the labeled toxin preparations for 15 min on ice and immediately analyzed by flow cytometry. The binding profiles were analyzed using Flowjo (Treestar).

#### Mammalian Cell Intoxication Assay

Cell-cycle arrest after typhoid toxin intoxication was examined by flow cytometry as previously described (Spanò et al., 2008). Briefly, after treatment with 6xHis-tagged typhoid toxin for 66 hr for Henle-407 or 18 hr for Jurkat cells, cells were trypsinized, collected, washed, and fixed for 2 hr in  $\sim 70\%$  ethanol/PBS at  $-20^{\circ}\text{C}$ . Fixed cells were washed with PBS and resuspended in  $500\ \mu\text{l}$  of PBS containing  $50\ \mu\text{g/ml}$  propidium iodide,  $0.1\ \text{mg/ml}$  RNase A,

and  $0.05\%$  Triton X-100. After incubation for 40 min at  $37^{\circ}\text{C}$ , cells were washed with PBS, resuspended in  $500\ \mu\text{l}$  PBS, filtered, and analyzed by a flow cytometry. The DNA content of treated cells was determined using Flowjo program (Treestar).

#### Mouse Intoxication Experiments

All mouse experiments were conducted according to protocols approved by Yale University's Institutional Animal Care and Use Committee. Age- and sex-matched 5- to 7-week-old C57BL/6 (wild-type), *Cmah*<sup>-/-</sup> (Jackson Laboratory), or *Cmah*<sup>19</sup> mice were intravenously injected with  $100\ \mu\text{l}$  solutions containing PBS alone, or either  $2\ \mu\text{g}$  or  $10\ \mu\text{g}$  of the indicated purified toxin preparations. Changes in behavior, weight, and survival of the toxin-injected mice were closely monitored and to minimize bias, blind end-point assessment was applied to all the experiments.

#### Blood Counting

Blood samples were collected by heart puncture 4.5 days after toxin treatment in Microtainer tubes coated with EDTA as an anticoagulant (BD), kept at room temperature, and analyzed within 2 hr after blood collection using a Hemavet 950FS hematology analyzer (Drew Scientific). Blood counts were analyzed by GraphPad Prism (GraphPad Software).



### Peripheral Blood Cell Preparation, Immunostaining, and Flow Cytometry Analysis

Peripheral blood samples of typhoid toxin-treated and control mice were collected into tubes coated with EDTA, incubated with 1 ml ACK buffer (BioWhittaker), incubated for 5 min, washed with 2 ml PBS, and centrifuged to collect peripheral blood leukocytes (PBLs). After a repetition of the red blood cell removal step, PBLs were washed, and were immediately incubated for 30 min on ice with 100  $\mu$ l of anti-mouse Ly-6G (Gr-1) antibody conjugated with FITC (eBioscience, 11-5931-81). PBLs were then washed with 2 ml of FACS buffer (PBS, 0.16% BSA), resuspended in 100  $\mu$ l FACS fixation buffer (PBS, 1% paraformaldehyde, 1% FCS), and used for flow cytometric analyses on BD accuri C6 (BD Biosciences). Peripheral blood samples from humans and chimpanzees were collected into EDTA tubes. Erythrocytes were separated from peripheral blood mononuclear cells (PBMC) by Ficol-Paque Plus. Erythrocytes in the PBMC layer were lysed by ACK buffer, and monocytes were removed by anti-CD14 beads (MACS Miltenyi Biotec).

### Typhoid Toxin Binding to Human, Chimpanzee, and Mouse Tissues

Cryosections of frozen tissue samples from human, chimpanzee and the different mouse strains, were overlaid with AF555-labeled wild-type typhoid toxin or the P1tB<sup>S35A</sup> mutant. After incubation in a covered humid chamber for 1 hr at room temperature, the slides were washed to remove nonbound toxins and the sections were fixed using 10% neutral buffered formalin. The nuclei were counterstained using Hoechst and the slides were washed and mounted in aqueous mounting media (VectaMount). Digital photomicrographs were taken using a Keyence BZ9000 fluorescence microscope (BIOREVO, BZ-9000, Keyence).

### Statistical Analysis

Two-tailed Student's *t* tests were performed in order to determine the statistical significance of experimental changes from control values. A *p* value < 0.05 was considered as statistically significant.

### SUPPLEMENTAL INFORMATION

Supplemental Information includes seven figures and two tables and can be found with this article online at <http://dx.doi.org/10.1016/j.cell.2014.10.057>.

### AUTHOR CONTRIBUTIONS

L.D. conducted or contributed to experiments shown in [Figures 1, 2, 3A, 3E, 5, S1, and S3](#) and [Tables 1 and S1](#). J.S. conducted or contributed to experiments shown in [Figures 1, 2B, 2D, 3B–3D, 3F–3H, 4A–4D, 6E, S2, S5, and S7](#) and [Tables 1 and S1](#). X.G. conducted experiments shown in [Figures 6A–6D, 6F, S4, and S6](#) and [Table S2](#). J.W. contributed to the analysis of the crystal structures. X.C. and H.Y. contributed to experiments shown in [Figure 1](#) and [Tables 1 and S1](#). N.V. planned, supervised, and interpret experiments shown in [Figures 5 and S3](#). Y.N.-M. contributed to experiments shown in [Figure 4D](#). J.E.G. and A.V. contribute to the design, interpretation, and supervision of this study. J.E.G. wrote the paper with input from A.V. and comments from all authors.

### ACKNOWLEDGMENTS

We thank Jonathon Okerblom for help with sialic acid analysis, Ana Lasic for assistance in the microscale thermophoresis studies, and members of the Galán laboratory for critical review of the manuscript. This work was supported by the National Cancer Institute (NCI) grant CA38701 to A.V. and National Institute of Allergy and Infectious Diseases (NIAID) grant AI079022 to J.E.G.

Received: August 8, 2014

Revised: September 9, 2014

Accepted: October 28, 2014

Published: December 4, 2014

### REFERENCES

- Adams, P.D., Afonine, P.V., Bunkóczy, G., Chen, V.B., Davis, I.W., Echols, N., Headd, J.J., Hung, L.-W., Kapral, G.J., Grosse-Kunstleve, R.W., et al. (2010). PHENIX: a comprehensive Python-based system for macromolecular structure solution. *Acta Crystallogr. D Biol. Crystallogr.* **66**, 213–221.
- Beddoe, T., Paton, A.W., Le Nours, J., Rossjohn, J., and Paton, J.C. (2010). Structure, biological functions and applications of the AB5 toxins. *Trends Biochem. Sci.* **35**, 411–418.
- Byres, E., Paton, A.W., Paton, J.C., Löfling, J.C., Smith, D.F., Wilce, M.C., Talbot, U.M., Chong, D.C., Yu, H., Huang, S., et al. (2008). Incorporation of a non-human glycan mediates human susceptibility to a bacterial toxin. *Nature* **456**, 648–652.
- Chou, H.H., Hayakawa, T., Diaz, S., Krings, M., Indriati, E., Leakey, M., Paabo, S., Satta, Y., Takahata, N., and Varki, A. (2002). Inactivation of CMP-N-acetylneuraminic acid hydroxylase occurred prior to brain expansion during human evolution. *Proc. Natl. Acad. Sci. USA* **99**, 11736–11741.
- Collaborative Computational Project, Number 4 (1994). The CCP4 suite: programs for protein crystallography. *Acta Crystallogr. D Biol. Crystallogr.* **50**, 760–763.
- Crump, J.A., and Mintz, E.D. (2010). Global trends in typhoid and paratyphoid Fever. *Clin. Infect. Dis.* **50**, 241–246.
- DeLano, W.L. (2002). The PyMOL Molecular Graphics System. <http://www.pymol.org>.
- Edsall, G., Gaines, S., Landy, M., Tigertt, W.D., Sprinz, H., Trapani, R.J., Mandel, A.D., and Benenson, A.S. (1960). Studies on infection and immunity in experimental typhoid fever. I. Typhoid fever in chimpanzees orally infected with *Salmonella typhosa*. *J. Exp. Med.* **112**, 143–166.
- Emsley, P., and Cowtan, K. (2004). Coot: model-building tools for molecular graphics. *Acta Crystallogr. D Biol. Crystallogr.* **60**, 2126–2132.
- Galán, J.E. (2001). *Salmonella* interactions with host cells: type III secretion at work. *Annu. Rev. Cell Dev. Biol.* **17**, 53–86.
- Haghjoo, E., and Galán, J.E. (2004). *Salmonella typhi* encodes a functional cytolethal distending toxin that is delivered into host cells by a bacterial-internalization pathway. *Proc. Natl. Acad. Sci. USA* **101**, 4614–4619.
- Hedlund, M., Tangvoranuntakul, P., Takematsu, H., Long, J.M., Housley, G.D., Kozutsumi, Y., Suzuki, A., Wynshaw-Boris, A., Ryan, A.F., Gallo, R.L., et al. (2007). N-glycolylneuraminic acid deficiency in mice: implications for human biology and evolution. *Mol. Cell. Biol.* **27**, 4340–4346.
- Ibarra, J.A., and Steele-Mortimer, O. (2009). *Salmonella*—the ultimate insider. *Salmonella* virulence factors that modulate intracellular survival. *Cell. Microbiol.* **11**, 1579–1586.
- Jacobsen, A., Hendriksen, R.S., Aaresturp, F.M., Ussery, D.W., and Friis, C. (2011). The *Salmonella enterica* pan-genome. *Microb. Ecol.* **62**, 487–504.
- McCoy, A.J., Grosse-Kunstleve, R.W., Adams, P.D., Winn, M.D., Storoni, L.C., and Read, R.J. (2007). Phaser crystallographic software. *J. Appl. Cryst.* **40**, 658–674.
- Metchnikoff, E., and Besredka, A. (1911). Recherches sur la fièvre typhoïde expérimentale. *Ann. Inst. Pasteur (Paris)* **25**, 865–874.
- Ohl, M.E., and Miller, S.I. (2001). *Salmonella*: a model for bacterial pathogenesis. *Annu. Rev. Med.* **52**, 259–274.
- Otwinowski, Z., and Minor, W. (1997). Processing of X-ray diffraction data collected in oscillation mode. *Methods Enzymol.* **276**, 307–326.
- Padler-Karavani, V., Hurtado-Ziola, N., Chang, Y.C., Sonnenburg, J.L., Ronaghy, A., Yu, H., Verhagen, A., Nizet, V., Chen, X., Varki, N., et al. (2014). Rapid evolution of binding specificities and expression patterns of inhibitory CD33-related Siglecs in primates. *FASEB J.* **28**, 1280–1293.
- Parkhill, J., Dougan, G., James, K.D., Thomson, N.R., Pickard, D., Wain, J., Churcher, C., Mungall, K.L., Bentley, S.D., Holden, M.T., et al. (2001). Complete genome sequence of a multiple drug resistant *Salmonella enterica* serovar Typhi CT18. *Nature* **413**, 848–852.

- Parry, C.M., and Threlfall, E.J. (2008). Antimicrobial resistance in typhoidal and nontyphoidal salmonellae. *Curr. Opin. Infect. Dis.* 21, 531–538.
- Parry, C.M., Hien, T.T., Dougan, G., White, N.J., and Farrar, J.J. (2002). Typhoid fever. *N. Engl. J. Med.* 347, 1770–1782.
- Raffatellu, M., Wilson, R.P., Winter, S.E., and Bäumlér, A.J. (2008). Clinical pathogenesis of typhoid fever. *J. Infect. Dev. Ctries.* 2, 260–266.
- Sabbagh, S.C., Forest, C.G., Lepage, C., Leclerc, J.M., and Daigle, F. (2010). So similar, yet so different: uncovering distinctive features in the genomes of *Salmonella enterica* serovars Typhimurium and Typhi. *FEMS Microbiol. Lett.* 305, 1–13.
- Schwan, W.R., Huang, X.Z., Hu, L., and Kopecko, D.J. (2000). Differential bacterial survival, replication, and apoptosis-inducing ability of *Salmonella* serovars within human and murine macrophages. *Infect. Immun.* 68, 1005–1013.
- Sixma, T.K., Pronk, S.E., Kalk, K.H., van Zanten, B.A., Berghuis, A.M., and Hol, W.G. (1992). Lactose binding to heat-labile enterotoxin revealed by X-ray crystallography. *Nature* 355, 561–564.
- Song, J., Gao, X., and Galán, J.E. (2013). Structure and function of the *Salmonella* Typhi chimaeric A(2)B(5) typhoid toxin. *Nature* 499, 350–354.
- Spanò, S., and Galán, J.E. (2012). A Rab32-dependent pathway contributes to *Salmonella typhi* host restriction. *Science* 338, 960–963.
- Spanò, S., Ugalde, J.E., and Galán, J.E. (2008). Delivery of a *Salmonella* Typhi exotoxin from a host intracellular compartment. *Cell Host Microbe* 3, 30–38.
- Spanò, S., Liu, X., and Galán, J.E. (2011). Proteolytic targeting of Rab29 by an effector protein distinguishes the intracellular compartments of human-adapted and broad-host *Salmonella*. *Proc. Natl. Acad. Sci. USA* 108, 18418–18423.
- Srikanth, C.V., Mercado-Lubo, R., Hallstrom, K., and McCormick, B.A. (2011). *Salmonella* effector proteins and host-cell responses. *Cell. Mol. Life Sci.* 68, 3687–3697.
- Tangvoranuntakul, P., Gagneux, P., Diaz, S., Bardor, M., Varki, N., Varki, A., and Muchmore, E. (2003). Human uptake and incorporation of an immunogenic nonhuman dietary sialic acid. *Proc. Natl. Acad. Sci. USA* 100, 12045–12050.
- Varki, N.M., Strobert, E., Dick, E.J., Jr., Benirschke, K., and Varki, A. (2011). Biomedical differences between human and nonhuman hominids: potential roles for uniquely human aspects of sialic acid biology. *Annu. Rev. Pathol.* 6, 365–393.
- Vladoianu, I.R., Chang, H.R., and Pechère, J.C. (1990). Expression of host resistance to *Salmonella typhi* and *Salmonella typhimurium*: bacterial survival within macrophages of murine and human origin. *Microb. Pathog.* 8, 83–90.
- Voetsch, A.C., Van Gilder, T.J., Angulo, F.J., Farley, M.M., Shallow, S., Marcus, R., Cieslak, P.R., Deneen, V.C., and Tauxe, R.V.; Emerging Infections Program FoodNet Working Group (2004). FoodNet estimate of the burden of illness caused by nontyphoidal *Salmonella* infections in the United States. *Clin. Infect. Dis.* 38 (Suppl 3), S127–S134.
- Waterman, S.R., and Holden, D.W. (2003). Functions and effectors of the *Salmonella* pathogenicity island 2 type III secretion system. *Cell. Microbiol.* 5, 501–511.
- Wienken, C., Baaske, P., Rothbauer, U., Braun, D., and Duhr, S. (2010). Protein-binding assays in biological liquids using microscale thermophoresis. *Nat. Commun.* 1, 100.